Title
Complexation and Redox Buffering of Iron(II) by Dissolved Organic Matter

Journal
Environmental Science and Technology, 51(19)

ISSN
0013-936X

Authors
Daugherty, Ellen E
Gilbert, Benjamin
Nico, Peter S
et al.

Publication Date
2017-10-03

DOI
10.1021/acs.est.7b03152

Peer reviewed

Complexation and Redox Buffering of Iron(II) by Dissolved Organic Matter

Ellen E. Daugherty[†], Benjamin Gilbert[*‡], Peter S. Nico[‡], and Thomas Borch[*†§]

[†] Department of Chemistry, Colorado State University, 1170 Campus Delivery, Fort Collins, Colorado 80523, United States

[‡] Energy Geoscience Division, Lawrence Berkeley National Laboratory, Berkeley, California 94720, United States

[§] Department of Soil and Crop Sciences, 1170 Campus Delivery, Fort Collins, Colorado 80523, United States

*(B.G.) Phone: 510-495-2748; fax: 510-486-5686; e-mail: bgilbert@lbl.gov., *(T.B.) Phone: 1-970-491-6235; fax: 970-491-5676; e-mail: thomas.borch@colostate.edu.

Abstract

Iron (Fe) bioavailability depends upon its solubility and oxidation state, which are strongly influenced by complexation with natural organic matter (NOM). Despite observations of Fe(II)–NOM associations under conditions favorable for Fe oxidation, the molecular mechanisms by which NOM influences Fe(II) oxidation remain poorly understood. In this study, we used X-ray absorption spectroscopy to determine the coordination environment of Fe(II) associated with NOM (as-received and chemically reduced) at pH 7, and investigated the effect of NOM complexation on Fe(II) redox stability. Linear combination fitting of extended X-ray absorption fine structure (EXAFS) data using reference organic ligands demonstrated that Fe(II) was complexed primarily by carboxyl functional groups in reduced NOM. Functional groups more likely to preserve Fe(II) represent much smaller fractions of NOM-bound Fe(II). Fe(II) added to anoxic solutions of as-received NOM oxidized to Fe(III) and remained organically complexed. Iron oxidation experiments revealed that the presence of reduced NOM limited Fe(II) oxidation, with over 50% of initial Fe(II) remaining after 4 h. These results suggest reduced NOM may preserve Fe(II) by functioning both as redox buffer and complexant, which may help explain the presence of Fe(II) in oxic circumneutral waters.

Introduction

Iron (Fe) is an essential micronutrient for both photosynthesis and respiration, and the two oxidation states of Fe can act as electron donors or acceptors for certain microbial metabolic pathways.(1, 2) Iron bioavailability can limit primary production in marine systems(3) and influence the biogeochemical functioning of soils and sediments. The bioavailability of Fe in aquatic environments is strongly affected by redox reactions that cycle Fe between +(II) and +(III) oxidation states and by complexation with organic ligands. Although free Fe(III) has very low solubility at circumneutral pH, organic complexation greatly increases solubility; over 99% of the pool of dissolved oceanic Fe(III) is organically complexed.(4) Fe(II) is far more

soluble than Fe(III), and free Fe(II) can reach high concentrations in reducing environments. However, Fe(II) is also readily complexed by NOM,(5) a reaction that may influence the redox behavior of Fe(II).

Both pure Fe(II) and mixed Fe(II)/Fe(III) species have been discovered in association with NOM in oxygen-rich aquatic environments. Examples include particles collected from the photic zone in the Southern Ocean,(6) from hydrothermal plumes at the midocean ridge East Pacific Rise (pH ~ 9),(7) and from freshwater lakes in New Jersey and Puerto Rico, U.S.(8) In addition, Sundman et al. identified mixed Fe(II)/Fe(III)–NOM complexes in streamwater and soil solutions in a boreal catchment at pH 4.3–5.8.(9) Such observations are contrary to expectations from simple models of Fe(II) oxidation rates and equilibrium calculations that show Fe(III) to be favored under oxic conditions at pH greater than 4. Several mechanisms have been suggested to explain the persistence of reduced Fe, including photochemical reduction,(10, 11) microbially mediated reduction,(2) and enhanced stability as a result of binding with organic ligands.(12)

Laboratory investigations of Fe–NOM oxidation–reduction chemistry have yielded contradictory results as to whether complexation of Fe by NOM enhances, inhibits, or has no effect upon the rate of Fe(II) oxidation. Such variability likely indicates that the effect of organic association on Fe(II) oxidation is dependent on the molecule and the experimental system. Tannic acid, gallic acid, and pyrogallol have been shown to inhibit Fe(II) oxidation, while salicylate and citrate enhance oxidation,(13, 14) and alanine and glutamic acid have no effect.(15) Studies using environmental samples show that NOM from different sources has variable effects on Fe(II) oxidation kinetics.(16-24) Most studies lack an explicit consideration of NOM redox activity(25, 26)and thorough characterization of binding interactions between Fe(II) and the chosen organic molecules. Natural organic matter is capable of acting as both an electron donor and acceptor, and can redox cycle repeatedly.(27) Aeschbacher et al. have shown that reducible moieties in NOM cover a wide range of standard reduction potentials, many of which can reduce Fe, and some of which may oxidize Fe.(28)

In this study, we used extended X-ray absorption fine structure (EXAFS) spectroscopy to determine the coordination environment of Fe(II) complexed by reduced NOM. Reduced NOM was used because Fe(II) underwent oxidation in the presence of as-received NOM. Recent EXAFS studies of the structure of Fe(III)–NOM compounds have shown that Fe(III) forms mononuclear complexes with NOM at low pH and Fe concentration and precipitates as Fe(III)–oxyhydroxides at higher pH and Fe content.(29) The mononuclear Fe(III) complexes involve chelate ring structures with carboxyl, hydroxamate, and hydroxyl groups.(30, 31) To our knowledge, there are no EXAFS studies of Fe(II) complexation by NOM and few works dedicated to elucidating the binding mechanisms in such complexes.(7, 8, 32) We also studied the consequences of NOM complexation on the rate of Fe(II) oxidation by O_2 for the standard Leonardite humic acid in order to improve

our current understanding of mechanisms controlling the fate and stability of Fe(II) in natural oxic waters.

Materials and Methods

Preparation of Samples and Standards

Samples for X-ray absorption spectroscopy analysis were prepared using dissolved natural organic matter (NOM) standards from the International Humic Substance Society (IHSS). These were chosen for their range of chemical properties and included Suwannee River fulvic acid (SRFA), humic acid (SRHA), and natural organic matter obtained by reverse osmosis (SRNOM); and Leonardite humic acid (LHA). Solutions were prepared in an anoxic glovebag by adding as-received NOM to O_2-free water and adjusting the pH to between 6.7 and 7.0 using 4 M NaOH (see Supporting Information (SI) Table S2 for exact pH values of NOM solutions).

As-received NOM was capable of oxidizing Fe(II) even under anoxic conditions. To ensure the preservation of ferrous Fe, we used the approach of Ratasuk and Nanny(33) to reduce some NOM samples by hydrogenation prior to addition of Fe. Reduction of 40–50 mg NOM in 2.75 mL of Millipore water was performed by gently bubbling H_2 gas through solution in the presence of 100 mg of Pd–Al_2O_3 catalyst for 24 h. Solutions were then anoxically transferred to centrifuge tubes and centrifuged at 6,000 rpm for 4.0 min to pellet out the catalyst. This process did not detectably change the solution pH.

Solutions of Fe(II) in the form of ferrous ammonium sulfate ($(NH_4)_2Fe(SO_4)_2{\cdot}6H_2O$), or Fe(III) in the form of ferric chloride ($FeCl_3$) were added to 1 mL of NOM solution to achieve 1–2 mM concentration and a 10–15 μmol Fe g^{-1} C ratio. The solution was mixed thoroughly, checked again for neutral pH, then lyophilized without exposure to oxygen. Samples were lyophilized in a vacuum flask, which was closed after drying and opened to atmospheric pressure in an anoxic glovebag. (Reduced samples are indicated with the subscript “red”.) Anoxic preparation and storage effectively prevented the oxidation of Fe(II) by oxygen—a control in which Fe(II) was added to anoxic water in the glovebag showed no evidence of Fe oxidation.

Samples of reference organic molecules were prepared in the same way as the as-received samples, using sodium citrate, pyrocatechol, 2,2′-bipyridine (2,2′-bipy), ethylenediamine (EDA), ethylenediaminetetraacetic acid (EDTA), and mercaptoethanol in place of NOM (SI Figure S1). High concentrations were used to minimize the Fe:C ratio and encourage Fe-ligand binding (SI Table S1).

The lyophilized samples were ground, if necessary, and packed densely into Teflon sample holders inside an anoxic glovebag. They were sealed with Kapton polyimide film and stored under anoxic conditions until transferred to the sample mount at the beamline. Preliminary experiments showed that

lyophilized samples were significantly less susceptible than solution samples to X-ray-induced oxidation of Fe(II) (SI Figure S2).

Data Collection and Analysis

X-ray Absorption Spectroscopy

All Fe K-edge X-ray absorption spectroscopic analyses were conducted at Beamline 11–2 at the Stanford Synchrotron Radiation Lightsource (SSRL) in Menlo Park, CA. Samples were mounted in an $N_{2\,(l)}$ cryostat to limit beam damage or oxidation. The Si(220) monochromator was detuned 50% to reduce higher order harmonics. Iron X-ray absorption near edge structure (XANES) and EXAFS fluorescence spectra were collected with a 100-element Ge detector simultaneously with the transmission spectrum of Fe foil, which was used for internal energy calibrations. Multiple scans per sample were acquired as necessary to achieve satisfactory data quality. A detector deadtime curve was collected for each beam time using a manganese filter.

Scans were calibrated by setting the first inflection point of the Fe(0) spectrum to 7112 eV, deadtime corrected, and averaged using SixPack software.(34) Background removal, normalization, and glitch removal at 7250 and 7600 eV were performed in Athena.(35) This program was also used to generate and qualitatively compare XANES, EXAFS, and Fourier transform spectra. First-shell fitting of Fourier transforms of the k^3-weighted EXAFS spectra was performed using IFFEFIT code in Artemis, using ferrihydrite as a standard. Fourier transform and k^3-weighted chi spectra were also used to create wavelet transforms using the Igor Pro wavelet transform script developed by Funke et al.(36) Wavelet transforms allow for the qualitative elemental discrimination of signal contributions from backscattering neighboring atoms. Linear combination fitting (LCF) of EXAFS spectra was performed in Artemis. Details of the linear combination fitting procedure can be found in the SI (see Figures S6 and S7).

Fe(II) Oxidation Experiments

The effect of Fe(II) binding by Leonardite humic acid (LHA) on the rate of Fe(II) oxidation by $O_2$was measured in aqueous solution. The initial solutions were prepared under anoxic conditions using O_2-purged Millipore water, reduced LHA, and $FeCl_2$. The Fe(II)–LHA sample was prepared with 2 mg/mL of reduced LHA and 0.79 mM Fe(II). Test samples showed that there was no detectable oxidation of Fe in any sample following the overnight incubation.

To start the experiment, samples were removed from the anoxic glovebag into open air and 1 mL was added into 30 mL glass beakers containing air-equilibrated solutions of 11 mL of 4.2 mM PIPES, a noncomplexing buffer, (37) at pH 7. To test whether PIPES affected the Fe(II) oxidation rate, the kinetics of Fe(II) oxidation were determined at 4.1 mM and 41 μM PIPES concentrations in the absence of LHA (SI Figure S8). Pseudo-first-order rate constants of Fe(II) oxidation were consistent with previously published values.(38, 39) While a difference was observed in the Fe(II) oxidation rates

between the two solutions, it was substantially smaller than the effect of adding reduced organic matter, and was likely a result of additions of NaOH required to maintain steady pH. Solutions were kept in the dark and stirred for the length of the oxidation experiments.

Iron(II) concentration as a function of time was determined by extracting 50-µL aliquots and immediately adding them to 150 µL of pH 7 PIPES-buffered, 50 mM solutions of 2,2′-bipyridine (2,2′-bipy).(40) After 30–60 s of reaction time, these solutions were analyzed by ultraviolet–visible (UV–vis) absorption spectroscopy. At some points, a duplicate 50 µL aliquot was taken, added to the 2,2′-bipy solution, capped, and stored in the dark for >30 min. The Fe(II) concentration was determined from the average intensity between 568 and 572 nm using a previously measured calibration curve.

Dissolved O_2 was measured simultaneously using the FOXY fiber optic probe (Ocean Optics). There was no detectable difference in the trend in dissolved O_2 between experiments with and without NOM (data not shown). We sought to quantify the generation of hydrogen peroxide (H_2O_2) by the Amplex red assay (A-22188, Molecular Probes, Invitrogen), but found the response to be significantly higher than expected when LHA_{red} was present. Although we were not able to obtain reliable H_2O_2 concentrations in the presence of organic matter, the assay confirmed the generation of this species, and data are shown in SI Figure S9.

The oxidizing capacity of as-received LHA was measured by adding Fe(II) to 1 mL of 2 mg/mL LHA to achieve a final Fe concentration of 1 mM. The reducing capacity of reduced LHA was measured by adding Fe(III) to 1 mL of 2 mg/mL LHA to achieve a final Fe concentration of 2 mM (SI Figure S10). All reactions were performed in an anoxic chamber. The concentration of Fe(II) was measured over 8 h using 2,2′-bipy but all redox reactions were completed within the first few minutes.

Results

XAS Data Analysis

The position of the absorption threshold of the Fe K-edge XANES spectra approximates the oxidation state of Fe (Figure 1). The Fe absorption edge for citrate + Fe(II) appeared at 7124 eV while that of citrate + Fe(III) appeared at a higher energy, 7126 eV. The spectra from all reference compounds with Fe(II) show no signs of oxidation. However, the edges of LHA + Fe(II) and SRFA + Fe(II) are very close to those of LHA + Fe(III) and citrate + Fe(III), clearly indicating that as-received NOM is capable of oxidizing Fe(II). In contrast, the spectra from reduced NOM samples are aligned with citrate + Fe(II), indicating preeminence of reduced Fe. Electron paramagnetic resonance (EPR) spectroscopy confirmed Fe(II) added to reduced NOM was not oxidized (SI Figure S3). The close agreement between the NOM + Fe(III) and the citrate + Fe(III) XANES spectra, as well as the EPR spectroscopy,

shows that oxidized Fe remains complexed by NOM and does not form precipitates.

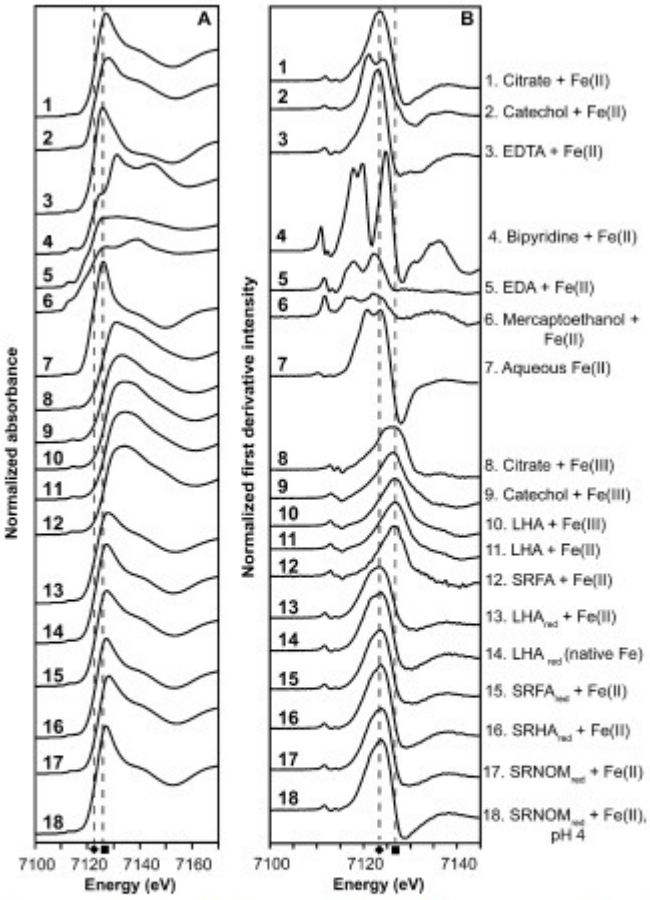

Figure 1. (A) Normalized Fe K-edge XANES spectra and (B) first derivatives of Fe-NOM samples and Fe−organic compound references at pH 7 unless indicated otherwise. NOM samples with added Fe have a 10−15 μmol Fe g^{-1} C ratio. Dotted lines show approximate E_0 values for citrate + Fe(II) (● 7124 eV) and citrate + Fe(III) (■ 7126 eV). The E_0 value represents the first well-defined peak in the first derivative.

First-shell fits of the Fe K-edge EXAFS data using a single-scattering oxygen path from ferrihydrite (SI Figure S5) provide information about the average coordination number (CN) and bond distances of Fe–O paths (Table 1). Complexes containing Fe(III) and Fe(II) added to as-received NOM have high CN values (≥6) compared to Fe(II) complexes with reduced NOM or O-containing organic reference ligands (5.0 ≤ CN ≤ 5.7). The bond distances for the Fe(III) complexes analyzed in this study range from 1.99–2.02 Å, typical values for Fe(III) octahedral coordination with oxygen in organic ligands.(41) The bond distances of the Fe(II) complexes range from 2.06 to 2.10 Å. Values above 2.08 Å are consistent with octahedrally coordinated Fe(II),(42-44) although path lengths that are shorter could indicate a mixture of Fe(II) and Fe(III).(45) The longer bond lengths for Fe–O/N complexation in reduced NOM−Fe(II) samples relative to Fe(III)–NOM samples indicate less

attraction between Fe(II) and the coordinating ligand and a weaker coordination environment.

Table 1. Bond Distances (R), Coordination Numbers (CN), and Debye-Waller Factors, (σ^2), Derived from Fourier Transform Fitting of the Fe−O Path in NOM Samples and Fe Citrate Complexes

sample information				first shell fitting parameters						
		dominant Fe oxidation								
OM type	OM redox state[b]	added	observed[a]	CN	error	R (Å)	error	σ^2 (Å^2)	error	R-factor
citrate	as-received	2	2	**5.4**	0.6	**2.10**	0.02	0.0052	0.0016	0.0218
citrate	as-received	3	3	**6.4**	0.7	**2.02**	0.01	0.0083	0.0018	0.0192
catechol	as-received	2	2	**5.6**	1.1	**2.08**	0.02	0.0094	0.0030	0.0493
LHA	reduced		2	**5.2**	0.6	**2.08**	0.01	0.0073	0.0018	0.0195
LHA	reduced	2	2	**5.0**	0.6	**2.06**	0.01	0.0087	0.0018	0.0175
LHA	as-received	2	3	**6.0**	0.6	**1.990**	0.009	0.0052	0.0012	0.0111
LHA	as-received	3	3	**6.1**	0.5	**1.989**	0.008	0.0052	0.0011	0.0108
SRFA	as-received	2	3	**6.6**	0.8	**2.01**	0.01	0.0042	0.0017	0.0271
SRFA	reduced	2	2	**5.0**	0.5	**2.07**	0.01	0.0073	0.0016	0.0180
SRHA	reduced	2	2	**5.5**	0.6	**2.08**	0.01	0.0076	0.0018	0.0262
SRNOM	reduced	2	2	**5.6**	0.5	**2.07**	0.009	0.0078	0.0013	0.0111
SRNOM	reduced, pH 4	2	2	**5.7**	0.5	**2.09**	0.009	0.0060	0.0012	0.0132

[a]Observed dominant Fe oxidation state is based on E_0 values, visual comparison of XANES spectra, and EPR results. [b]All samples are at pH 7 unless otherwise indicated.

Wavelet transform (WT) analysis was employed to investigate the nature of the atoms beyond the first coordination shell. WT analysis uses a two-dimensional plot created from the *k*-weighted EXAFS spectrum and the corresponding Fourier transform to determine the distance and scattering strength of atoms. As can be seen in the WT plot for ferrihydrite in Figure 2, second shell Fe contributes a strong feature at about 7 Å^{-1} and 2.75 Å. This feature is absent from WT plots for all complexes of Fe and NOM, demonstrating there is no significant presence of multinuclear Fe clusters or precipitates. Similar observations have been reported for systems containing low concentrations of Fe(III) at low to neutral pH.(29, 46, 47)

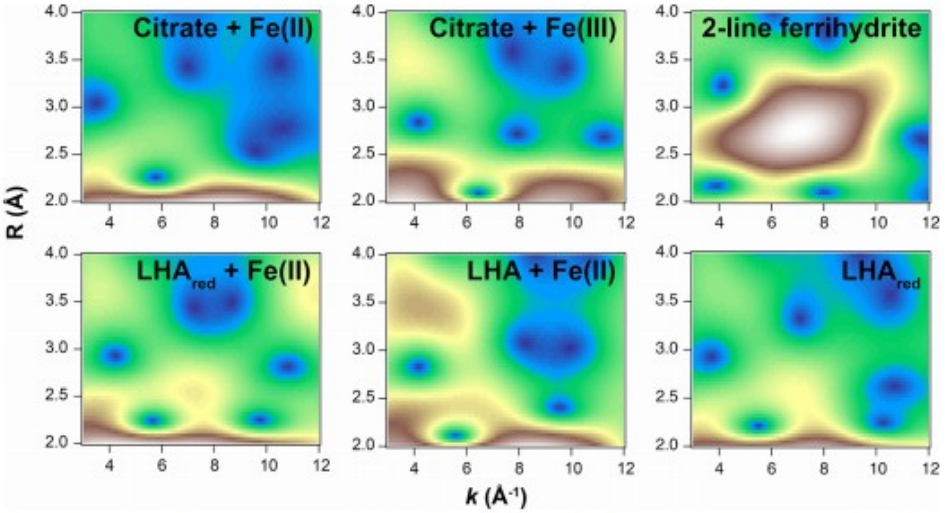

Figure 2. Wavelet transform moduli displaying the second and third coordination shells (Morlet wavelet parameters: $\eta = 9$, $\sigma = 1$) of Fe−organic complexes and ferrihydrite. LHA is Leonardite humic acid.

Linear combination fitting (LCF) of Fe EXAFS organic reference spectra to reduced NOM spectra reveals the dominant types of complexes formed

(Figure 3). The strong contribution from the citrate + Fe(II) reference shows 50–75% of Fe was bound by carboxyl and possibly hydroxyl groups.
(42) Optimal fits to nearly all sample spectra required small contributions from catechol and EDTA. In $SRHA_{red}$ + Fe(II) and $SRNOM_{red}$ + Fe(II) at pH 4, nearly 20% of the Fe exists as hydrated Fe(II), which may represent solvation complexes or outer-sphere complexes, as these are likely indistinguishable. Fe(III)–organic reference complexes (i.e., citrate + Fe(III) or catechol + Fe(III)) were fit, to varying degrees (5–25%), to every sample except $SRNOM_{red}$ + Fe(II) at pH 4. Though nitrogen- and sulfur-containing organic compounds generally have a higher affinity for Fe(II) than oxygen-containing groups,(48) they represent a small proportion of the NOM types studied (0.5–2% by weight), and LCF analysis did not reveal any contributions from amine-only or thiol ligands (as determined from ethylenediamine + Fe(II) and mercaptoethanol + Fe(II) references). Bipyridine-like and EDTA-like functional groups, both of which contain nitrogen, were found to complex 5–20% of the Fe (as Fe(II)) in $SRFA_{red}$ + Fe(II), $SRNOM_{red}$ + Fe (II), LHA_{red} + Fe(II), and LHA_{red}. Consistent with the WT analyses, LCF results indicate the absence of significant quantities of polymeric Fe in the reduced NOM samples.

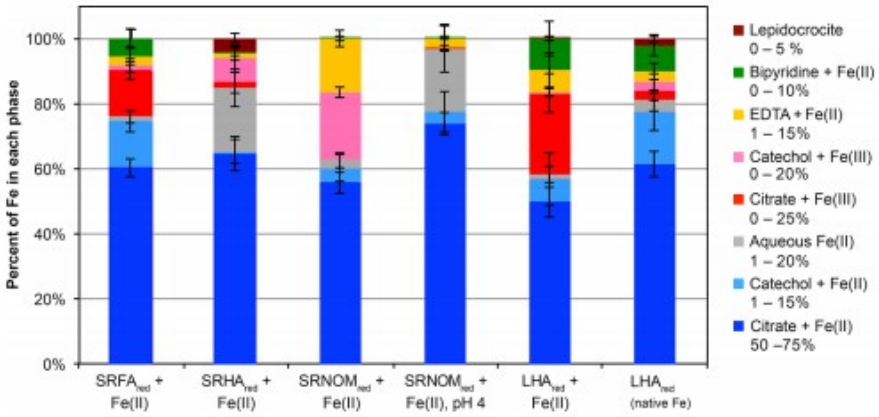

Figure 3. Weights of Fe references in linear combination fits of k^3-weighted Fe EXAFS for Fe in reduced NOM complexes (pH 7 unless indicated otherwise). Values shown are the averages of the top 10 combinatorial fits, and error bars represent the standard deviations or the average of the errors given by the fit, whichever is larger. Percentages shown under each legend heading represent the range of that reference present in all the samples.

Fe(II) Oxidation Experiments

To observe the effect of Fe–NOM complexation on iron redox speciation during oxidation by O_2, we exposed a pH 7 buffered anoxic solution of LHA_{red} + Fe(II) to atmospheric and dissolved $O_2$for over 3 h. The extent of Fe(II) oxidation decreased substantially in the presence of LHA_{red}compared to a NOM-free control (Figure 4). While total oxidation of Fe(II) without LHA_{red} occurred within about 110 min, over 50% of the Fe(II) associated with LHA_{red} remained reduced after 4 h of exposure to O_2. Fe(II) assays performed on samples stored in the dark for 30 min had approximately a third higher Fe(II) concentrations than those performed immediately following sampling, suggesting that some of the Fe(III) formed through the reaction of Fe(II) and

O_2 was re-reduced once open air was excluded via capping. The remaining sample was analyzed for Fe(II) the subsequent day, but no residual Fe(II) was detectable at that point. The exposure of LHA_{red} to O_2 generated hydrogen peroxide (H_2O_2), indicating O_2 directly reacted with redox-active moieties (SI Figure S9). In the presence of Fe(II), the measured levels of H_2O_2 were suppressed.

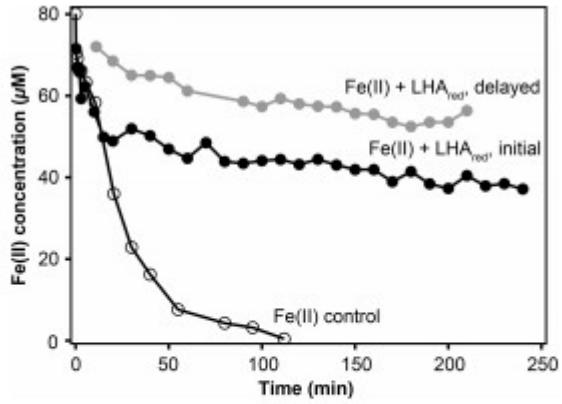

Figure 4. Experimental data from Fe(II) oxidation experiments with 67 μM Fe(II), 0.17 mg/mL LHA_{red}, and 4.16 mM PIPES and Fe(II) control data (80 μM Fe(II), 4.16 mM PIPES). The "Fe(II) + LHA_{red}, initial" measurements were made on aliquots immediately after the addition of a dye (2,2′-bipyridine), a colorimetric assay for iron(II), while the "Fe(II) + LHA_{red}, delayed" measurements were made 30 or more minutes after addition of the dye and storage in the dark.

Discussion

Complexation with organic matter has often been proposed to alter the rate of Fe(II) oxidation—potentially leading to long-term preservation of Fe(II) in oxic circumneutral environments—yet little research has been dedicated to understanding Fe(II)–OM complexation. In this study, we investigated Fe(II) complexation with organic matter using Fe K-edge spectroscopy and determined the impact of reduced organic matter on Fe(II) oxidation.

Oxidation of Fe(II) by As-Received LHA

Due to published observations of humic substances reducing Fe(III)(49, 50) and preserving added Fe(II),(32) we expected Fe(II) to remain reduced when added to as-received NOM in anoxic water. Instead, we observed overwhelming oxidation of Fe(II) when added to LHA at pH 7 (SI Figure S3). Based on electrochemical studies performed by Aeschbacher et al., a small proportion (~8%) of the reducible moieties in LHA have standard reduction potentials greater than that for the $Fe(OH)_3/Fe^{2+}$ redox couple (0.062 V).(28) At the low Fe:LHA ratio present in our samples, these groups outnumber the amount of added Fe(II) and are likely responsible for oxidation of added Fe(II). Although the identities of these functional groups are unknown, they could include semiquinone radicals, which have been shown to oxidize As(III) under anoxic conditions and are proposed to oxidize Fe(II) following irradiation of SRFA.(26, 51) As a result of Fe(II) oxidation in the presence of

as-received NOM, we chose to investigate Fe(II)–NOM complexation using chemically reduced NOM.

Fe(II)–NOM Complexation

We expected complexation between Fe(II) and N- and S-containing functional groups to predominate because some of the strongest Fe(II) ligands contain N or S,(48) and moles of organic N and S are 1–2 orders of magnitude greater than moles of added Fe(II) in our samples.(52) However, our EXAFS fitting results show that these two elements have low or no representation in the formed Fe(II)–NOM complexes. Instead, approximately 75–100% of Fe(II) added to reduced organic matter remained reduced and formed mononuclear oxygen-containing complexes (Figures 2 and 3). Citrate, which complexes Fe(II) through carboxyl and hydroxyl functional groups,(42) better represents the predominant type of complexing ligand than any other reference used, as determined from LCF analysis of the Fe K-edge EXAFS (Figure 3). This result generally supports the equilibrium modeling approach used by Catrouillet et al., which indicated that Fe(II) added to LHA was primarily bound in bidentate complexes with carboxyl groups at acidic to neutral pH.(32) Hence, Fe(II) binding to NOM appears largely analogous to Fe(III)–NOM complexes, but weaker, as indicated by Fe(II) complexation kinetics studies.(22) EXAFS studies of NOM bound to ferric iron indicated mononuclear, bidentate coordination of Fe(III) with oxygen or nitrogen and specific coordination with carboxylate functional groups.(29, 30, 45, 46, 53) Since citrate has been shown to accelerate Fe(II) oxidation,(13, 14, 54) this type of complexation is unlikely to preserve Fe(II) in oxic environments.

While our results support the assertion that the majority of Fe(II) is complexed to carboxyl groups at neutral pH, this type of interaction does not explain the full complexity and extent of Fe(II)–NOM interactions (Figure 3). Though contributions from the remaining ligands are less definite than that of citrate; catechol-, EDTA-, and bipyridine-like complexation may account for up to 30% of the Fe in these Fe(II)–NOM mixtures. Catechol and EDTA form more stable complexes with Fe(III) than Fe(II),(48) so complexation with ligands similar to these may be unlikely to preserve Fe(II). However, phenols like catechol are potentially redox-active moieties in NOM capable of reducing, or preventing the net oxidation of, associated Fe. Phenols and polyphenols may therefore contribute to Fe(II) preservation, as has been shown with tannic acid, a polyphenol, which preserved Fe(II) for over 100 h in the presence of oxygen.(13) Complexation with pyridinic functional groups as found in 2,2′-bipyridine and 1,10-phenanthroline could potentially prevent oxidation of Fe(II) because tris complexes with these ligands thermodynamically stabilize Fe(II) over Fe(III).(55, 56) Pyridinic nitrogen represents a very low proportion of functional groups in NOM—elemental N is only 1% of NOM by weight and only 20–35% of that is pyridinic N.(52, 57)Therefore, the likelihood of three pyridinic functional groups coming together to bind with Fe(II) and form a tris complex is low.

It remains unclear why Fe(II) is not bound to high-affinity N and S sites at the expected levels. At pH 7, deprotonated carboxyl groups greatly outnumber N, S, and added Fe(II) for the NOM investigated, so their relatively high abundance may account for the prevalence of Fe(II)-carboxyl complexation.(58) Another possible explanation is that complexation with these functional groups occurs at a slower rate, with carboxyl groups complexing Fe(II) more rapidly. Over longer periods, Fe(II) may exchange to lower abundance, higher affinity functional groups, such as N- or S-containing moieties. Such complexation may promote long-term stabilization of Fe(II). Longer-term equilibration studies will be required to determine whether Fe(II) exchanges to lower abundance functional groups and if so, whether these complexes inhibit Fe(II) oxidation.

These results differ from the few published studies that investigated Fe(II)-NOM interactions at the molecular level, none of which targeted Fe(II) complexation using Fe K-edge EXAFS spectroscopy. Toner et al. used scanning transmission X-ray microscopy (STXM) to map the distribution of Fe(II) and different types of carbon in particles collected from a sulfide-rich hydrothermal plume.(7) Based on their results and published stability constant data, the authors suggested organo-sulfur compounds were responsible for preserving Fe(II) after exposure to oxygen. In contrast, the NOM types used in our study do not come from sulfur-rich environments, and therefore have low percentages of sulfur.(52) Fe(II)–thiol complexation was consistently excluded from our samples by linear combination fits based on the use of a Fe(II)–mercaptoethanol reference. In another recent study, von der Heyden et al. concluded that Fe(II)-containing particles from marine and lacustrine samples were more likely to have alcohol, carboxamide, and/or carbonate C than Fe(III)-containing particles.(8) In contrast to the work presented here, both prior studies show only a correlation between the presence of Fe(II) and certain types of organic matter—they do not directly probe the coordination environment of Fe(II)–organic complexes.

Differences in NOM source and type were expected to influence Fe(II) complexation, however, our data show that they have small and unpredictable effects. The NOM samples chosen for this study exhibit substantial chemical variation. SRFA has a higher oxygen content, and is more aliphatic and monosaccharide-rich while LHA is highly aromatic and has a lower acidity.(52, 59) Consistent with the higher carboxylic and phenolic acidity of SRFA, added Fe(II) forms complexes with more citrate- and catechol-like groups in $SRFA_{red}$ than LHA_{red} (Figure 3). This correlation with chemical characteristics does not appear to hold true for the native Fe(II) in LHA_{red}, which is complexed by citrate- and catechol-like groups in approximately equal proportion to Fe(II) added to $SRFA_{red}$.

Since NOM and Fe can be protonated and hydroxylated, respectively, pH has a substantial impact on Fe–NOM complexation. LCF analysis of Fe(II) + $SRNOM_{red}$ at pH 4 and 7 demonstrates that higher solution acidity promotes the preservation of Fe(II) over Fe(III) but also limits organic complexation

(Figure 3). At low pH, the oxidation of Fe(II) is slower(12) and Fe(II) is thermodynamically favored at a wider range of Eh values.(60) At pH 4, more carboxyl groups are protonated than at pH 7, resulting in fewer available binding sites, leading to a higher proportion of hydrated Fe (fit by “aqueous Fe(II)”). These results are consistent with the findings of Catrouillet et al., which showed a decreasing proportion of LHA-bound Fe(II) with decreasing pH from 8 to 3.(32)

Effect of LHA_{red} on Fe(II) Oxidation

During oxidation by O_2, reduced NOM maintained a steady-state concentration of Fe(II) over the course of several hours through what appears to be a redox buffering mechanism (Figure 4). During this process, LHA_{red} was oxidized—a reaction likely catalyzed by native Fe or semiquinones(25, 61)—resulting in the net production of LHA_{ox} and H_2O_2 (SI Figure S9).

$$LHA_{red} + O_2 \rightarrow LHA_{ox} + H_2O_2 \quad (1)$$

Along with O_2, H_2O_2 can oxidize Fe(II) in a Fenton-like reaction to form Fe(III)–LHA, OH^- and $OH^\bullet$. The occurrence of this reaction is supported by the suppression of the H_2O_2 concentration in the Fe(II)−LHA_{red} sample (SI Figure S9).

$$O_2 + Fe^{(II)}LHA \rightleftharpoons O_2^{\bullet-} + Fe^{(III)}LHA \quad (2)$$

$$H_2O_2 + Fe^{(II)}LHA \rightarrow OH^- + OH^\bullet + Fe^{(III)}LHA \quad (3)$$

Delayed Fe(II) measurements showed a ~34% increase in Fe(II) concentration when aliquots of the reaction mixture were stored in airtight containers for over 30 min prior to Fe(II) measurement (Figure 4), suggesting LHA_{red} re-reduced newly formed Fe(III). This explanation is supported by the results of Bauer and Kappler, who observed humic substances reducing Fe(III), even as they were being oxidized by O_2.(50) Superoxide ($O_2^{\bullet-}$) has been shown to reduce Fe(III)–NOM complexes(62) and may also contribute to re-reduction of Fe(III).

$$LHA_{red} + Fe(III)LHA \rightarrow LHA_{ox} + Fe(II)LHA \quad (4)$$

This redox buffering process may explain the persistence of 50% of the initial Fe(II) after 4 h under oxic conditions. Calculations based on our measurement of the Fe(III)-reducing capacity of LHA_{red}(SI Figure S10) demonstrate that LHA in this system can reduce the total concentration of Fe about 1.6 times. A proposed scheme in Figure 5 summarizes the key reactions supported by our findings.

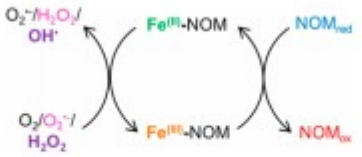

Figure 5. Simplified proposed reaction scheme showing Fe redox cycling in the presence of reduced organic matter and oxygen.

Though it is evident that reducing groups in LHA_{red} contribute to the prolonged existence of Fe(II) under oxic conditions, the identities of these groups—in our system—remain unclear. Quinones are responsible for much of the redox behavior of NOM, and our results bear similarities to observations of coupled Fe-quinone cycling. Hydroquinones, which form during reduction via hydrogenation,(33) can rapidly reduce Fe(III) to Fe(II), outcompeting reoxidation of Fe(II) to Fe(III)(63) by molecular oxygen or reactive oxygen species. Natural organic matter itself appears to be even more adept at cycling Fe than individual quinones. For instance, results published by Jiang et al. show SRFA cycling Fe at rates 10–100 times faster than 1,4-hydroquinone at pH 4.(25)However, our NOM reduction method using H_2–Pd/Al_2O_3 at pH 7 is similar to the one used by Ratasuk and Nanny, which they claimed removed quinone groups via hydrogenolysis.(33) They concluded that the redox active groups responsible for electron transfer under this reduction treatment must be nonquinone moieties, such as thiols and nitrogen functional groups. Therefore, further work is necessary to identify the reducing groups active under the conditions used in this study. In addition, the extent to which Fe(II) complexation affects the Fe(II) oxidation rate and steady-state concentration is not easily discernible and requires further investigation.

Environmental Implications

Our findings clarify important roles of NOM in Fe(II) speciation and Fe redox cycling. Under circumneutral reducing conditions, NOM readily binds low concentrations of Fe(II), primarily forming mononuclear complexes with citrate-like groups. Although additional complexation modes are also identified, for these experiments, the distribution of complexing ligands appears to be determined mostly by abundance rather than expected affinities. The observed Fe(II)–NOM complexes are likely important forms of bioavailable Fe(II) for microorganisms, thereby influencing Fe cycling and primary productivity.

None of the principal ligands observed for Fe(II) are known to thermodynamically stabilize the reduced state. However, the addition of O_2 to Fe(II)–NOM mixtures initiates a dynamic redox cycle that sustains a steady state concentration of Fe(II) for several hours longer than Fe(II) without NOM. Although the redox buffering mechanism does not explain the long term stabilization of Fe(II), it is likely to occur in the surface waters of streams, lakes, and oceans subjected to diurnal photoredox cycles and in

domains of soils and sediments subjected to cycles in microbial metabolisms capable of reducing NOM.(10, 64, 65)

The experimental conditions used in this study were chosen to facilitate the identification of Fe(II)–NOM complexes using XAS spectroscopy and do not represent the full range of possible environmental conditions. Competition from other divalent cations, a higher Fe:NOM ratio in some environments, and the presence of unreduced NOM will limit the iron complexation and redox buffering capabilities of NOM. Additional work will be required to confirm that the Fe(II)–NOM interactions observed in these laboratory studies are reproduced in naturally reduced soils and sediments.

Acknowledgment

Use of the Stanford Synchrotron Radiation Lightsource, SLAC National Accelerator Laboratory, is supported by the U.S. Department of Energy, Office of Science, Office of Basic Energy Sciences under Contract No. DE-AC02-76SF00515. We thank R. Davis for his beamline support at the synchrotron and Andreas Kappler for advice on the H_2 reduction method. EPR measurements were performed using EMSL, a DOE Office of Science User Facility sponsored by the Office of Biological and Environmental Research and located at Pacific Northwest National Laboratory. This material is based upon work that is supported by the National Institute of Food and Agriculture, U.S. Department of Agriculture, under award number 2013-67019-21359 and, in part, by a National Science Foundation (NSF) Award (EAR 1451494) to T.B. Work by B.G. and P.S.N. was supported as part of the Watershed Function Scientific Focus Area funded by the U.S. Department of Energy, Office of Science, Office of Biological and Environmental Research under Award Number DE-AC02-05CH11231.

References

(1) Weber, K. A.; Achenbach, L. A.; Coates, J. D. Microorganisms pumping iron: anaerobic microbial iron oxidation and reduction. Nat. Rev. Microbiol. 2006, 4, 752−764. (2) Melton, E. D.; Swanner, E. D.; Behrens, S.; Schmidt, C.; Kappler, A. The interplay of microbially mediated and abiotic reactions in the biogeochemical Fe cycle. Nat. Rev. Microbiol. 2014, 12, 797−809. (3) Boyd, P. W.; Jickells, T.; Law, C. S.; Blain, S.; Boyle, E. A.; Buesseler, K. O.; Coale, K. H.; Cullen, J. J.; de Baar, H. J. W.; Follows, M.; et al. Mesoscale iron enrichment experiments 1993−2005: Synthesis and future directions. Science 2007, 315, 612−617. (4) Rue, E. L.; Bruland, K. W. Complexation of iron(III) by natural organic ligands in the Central North Pacific as determined by a new competitive ligand equilibration/adsorptive cathodic stripping voltammetric method. Mar. Chem. 1995, 50, 117−138. (5) Yamamoto, M.; Nishida, A.; Otsuka, K.; Komai, T.; Fukushima, M. Evaluation of the binding of iron(II) to humic substances derived from a compost sample by a colorimetric method using ferrozine. Bioresour. Technol. 2010, 101, 4456−4460. (6) von der Heyden, B. P.; Roychoudhury, A. N.; Mtshali, T. N.; Tyliszczak, T.; Myneni, S. C. B. Chemically and geographically distinct solid-phase iron pools in the

Southern Ocean. Science 2012, 338, 1199−1201. (7) Toner, B. M.; Fakra, S. C.; Manganini, S. J.; Santelli, C. M.; Marcus, M. A.; Moffett, J. W.; Rouxel, O.; German, C. R.; Edwards, K. J. Preservation of iron(II) by carbon-rich matrices in a hydrothermal plume. Nat. Geosci. 2009, 2, 197−201. (8) von der Heyden, B. P.; Hauser, E. J.; Mishra, B.; Martinez, G. A.; Bowie, A. R.; Tyliszczak, T.; Mtshali, T. N.; Roychoudhury, A. N.; Myneni, S. C. B. Ubiquitous Presence of Fe(II) in Aquatic Colloids and Its Association with Organic Carbon. Environ. Sci. Technol. Lett. 2014, 1, 387−392. (9) Sundman, A.; Karlsson, T.; Laudon, H.; Persson, P. XAS study of iron speciation in soils and waters from a boreal catchment. Chem. Geol. 2014, 364, 93−102. (10) Voelker, B. M.; Morel, F. M. M.; Sulzberger, B. Iron Redox Cycling in Surface Waters: Effects of Humic Substances and Light. Environ. Sci. Technol. 1997, 31, 1004−1011. (11) Barbeau, K.; Rue, E. L.; Bruland, K. W.; Butler, A. Photochemical cycling of iron in the surface ocean mediated by microbial iron(III)-binding ligands. Nature 2001, 413, 409−413. (12) Millero, F. J.; Sotolongo, S.; Izaguirre, M. The oxidation kinetics of Fe(II) in seawater. Geochim. Cosmochim. Acta 1987, 51, 793−801. (13) Theis, T. L.; Singer, P. C. Complexation of iron(II) by organic matter and its effect on iron(II) oxidation. Environ. Sci. Technol. 1974, 8, 569−573. (14) Pham, A. N.; Waite, T. D. Modeling the kinetics of Fe(II) oxidation in the presence of citrate and salicylate in aqueous solutions at pH 6.0−8.0 and 25 degrees C. J. Phys. Chem. A 2008, 112, 5395− 5405. (15) Santana-Casiano, J. M.; Gonzalez-Da´ vila, M.; Rodríguez, M. J.;´ Millero, F. J. The effect of organic compounds in the oxidation kinetics of Fe(II). Mar. Chem. 2000, 70, 211−222. (16) Jobin, R.; Ghosh, M. M. Effect of buffer intensity and organic matter on the oxygenation of ferrous iron. J. Am. Water Works Assoc. 1972, 64, 590−595. (17) Pullin, M. J.; Cabaniss, S. E. The effects of pH, ionic strength, and iron−fulvic acid interactions on the kinetics of non-photochemical iron transformations. I. Iron(II) oxidation and iron(III) colloid formation. Geochim. Cosmochim. Acta 2003, 67, 4067−4077. (18) Davison, W.; Seed, G. The kinetics of the oxidation of ferrous iron in synthetic and natural waters. Geochim. Cosmochim. Acta 1983, 47, 67−79. (19) Emmenegger, L.; King, D. W.; Sigg, L.; Sulzberger, B. Oxidation Kinetics of Fe(II) in a Eutrophic Swiss Lake. Environ. Sci. Technol. 1998, 32, 2990−2996. (20) Craig, P. S.; Shaw, T. J.; Miller, P. L.; Pellechia, P. J.; Ferry, J. L. Use of multiparametric techniques to quantify the effects of naturally occurring ligands on the kinetics of Fe(II) oxidation. Environ. Sci. Technol. 2009, 43, 337−342. (21) Rose, A. L.; Waite, T. D. Kinetic model for Fe(II) oxidation in seawater in the absence and presence of natural organic matter. Environ. Sci. Technol. 2002, 36, 433−444. (22) Rose, A. L.; Waite, T. D. Kinetics of iron complexation by dissolved natural organic matter in coastal waters. Mar. Chem. 2003, 84, 85−103. (23) Rose, A. L.; Waite, T. D. Effect of dissolved natural organic matter on the kinetics of ferrous iron oxygenation in seawater. Environ. Sci. Technol. 2003, 37, 4877−4886. (24) Bligh, M. W.; Waite, T. D. Role of heterogeneous precipitation in determining the nature of products formed on oxidation of Fe(II) in seawater containing natural organic matter. Environ. Sci. Technol. 2010, 44, 6667−6673. (25) Jiang, C.; Garg, S.;

Waite, T. D. Hydroquinone-Mediated Redox Cycling of Iron and Concomitant Oxidation of Hydroquinone in Oxic Waters under Acidic Conditions: Comparison with Iron−Natural Organic Matter Interactions. Environ. Sci. Technol. 2015, 49, 14076− 14084. (26) Garg, S.; Jiang, C.; Waite, T. D. Mechanistic insights into iron redox transformations in the presence of natural organic matter: Impact of pH and light. Geochim. Cosmochim. Acta 2015, 165, 14−34. (27) Klü pfel, L.; Piepenbrock, A.; Kappler, A.; Sander, M. Humic substances as fully regenerable electron acceptors in recurrently anoxic environments. Nat. Geosci. 2014, 7, 195−200. (28) Aeschbacher, M.; Vergari, D.; Schwarzenbach, R. P.; Sander, M. Electrochemical analysis of proton and electron transfer equilibria of the reducible moieties in humic acids. Environ. Sci. Technol. 2011, 45, 8385−8394. (29) Karlsson, T.; Persson, P.; Skyllberg, U.; Mö rth, C.-M.; Giesler, R. Characterization of iron(III) in organic soils using extended X-ray absorption fine structure spectroscopy. Environ. Sci. Technol. 2008, 42, 5449−5454. (30) Karlsson, T.; Persson, P. Complexes with aquatic organic matter suppress hydrolysis and precipitation of Fe(III). Chem. Geol. 2012, 322−323, 19−27. (31) Mikutta, C.; Kretzschmar, R. Spectroscopic evidence for ternary complex formation between arsenate and ferric iron complexes of humic substances. Environ. Sci. Technol. 2011, 45, 9550−9557. (32) Catrouillet, C.; Davranche, M.; Dia, A.; Bouhnik-Le Coz, M.; Marsac, R.; Pourret, O.; Gruau, G. Geochemical modeling of Fe(II) binding to humic and fulvic acids. Chem. Geol. 2014, 372, 109−118. (33) Ratasuk, N.; Nanny, M. A. Characterization and quantification of reversible redox sites in humic substances. Environ. Sci. Technol. 2007, 41, 7844−7850. (34) Webb, S. M. SIXPack: A Graphical User Interface for XAS Analysis Using IFEFFIT. Phys. Scr. 2005, T115, 1011−1014. (35) Ravel, B.; Newville, M. ATHENA, ARTEMIS, HEPHAESTUS: data analysis for X-ray absorption spectroscopy using IFEFFIT. J. Synchrotron Radiat. 2005, 12, 537−541. (36) Funke, H.; Scheinost, A.; Chukalina, M. Wavelet analysis of extended x-ray absorption fine structure data. Phys. Rev. B: Condens. Matter Mater. Phys. 2005, 71, 94110. (37) Yu, Q.; Kandegedara, A.; Xu, Y.; Rorabacher, D. B. Avoiding Interferences from Good’s Buffers: A Contiguous Series of Noncomplexing Tertiary Amine Buffers Covering the Entire Range of pH 3−11. Anal. Biochem. 1997, 253, 50−56. (38) Pham, A. N.; Waite, T. D. Oxygenation of Fe(II) in the Presence of Citrate in Aqueous Solutions at pH 6.0−8.0 and 25 °C: Interpretation from an Fe(II)/Citrate Speciation Perspective. J. Phys. Chem. A 2008, 112, 643−651. (39) Santana-Casiano, J. M.; Gonzalez-Da´ vila, M.; Millero, F. J.´ Oxidation of nanomolar levels of Fe(II) with oxygen in natural waters. Environ. Sci. Technol. 2005, 39, 2073−2079. (40) Moss, M. L.; Mellon, M. G. Colorimetric Determination of Iron with 2,2′-Bipyridyl and with 2,2′,2′-Terpyridyl. Ind. Eng. Chem., Anal. Ed. 1942, 14, 862−865. (41) Saines, P. J.; Yeung, H. H.-M.; Hester, J. R.; Lennie, A. R.; Cheetham, A. K. Detailed investigations of phase transitions and magnetic structure in Fe(III), Mn(II), Co(II) and Ni(II) 3,4,5- trihydroxybenzoate (gallate) dihydrates by neutron and X-ray diffraction. Dalt. Trans. 2011, 40, 6401−6410. (42) Strouse, J.; Layten, S. W.; Strouse, C. E. Structural Studies

of Transition Metal Complexes of Triionized and Tetraionized Citrate. Models for the Coordination of the Citrate Ion to Transition Metal Ions in Solution and at the Active Site of Aconitase. J. Am. Chem. Soc. 1977, 99, 562−572. (43) Lundberg, D.; Ullstrom, A.-S.; D'Angelo, P.; Persson, I. A structural study of the hydrated and the dimethylsulfoxide, N,N′- dimethylpropyleneurea, and N,N -dimethylthioformamide solvated iron(II) and iron(III) ions in solution and solid state. Inorg. Chim. Acta 2007, 360, 1809−1818. (44) Yang, X.; Li, J.; Zhao, X.-H.; Wang, H.-W.; Shan, Y.-K. Hydrogen bonding and π-π stacking in the three-dimensional supramolecular complex bis(4,4′-bipyridinium) diaquadioxalatoferrate (II) bis(hydrogen oxalate). Acta Crystallogr., Sect. C: Cryst. Struct. Commun. 2007, 63, m171−3. (45) van Schaik, J. W. J.; Persson, I.; Kleja, D. B.; Gustafsson, J. P. EXAFS study on the reactions between iron and fulvic acid in acid aqueous solutions. Environ. Sci. Technol. 2008, 42, 2367−2373. (46) Karlsson, T.; Persson, P. Coordination chemistry and hydrolysis of Fe(III) in a peat humic acid studied by X-ray absorption spectroscopy. Geochim. Cosmochim. Acta 2010, 74, 30−40. (47) Sjö stedt, C.; Persson, I.; Hesterberg, D.; Kleja, D. B.; Borg, H.; Gustafsson, J. P. Iron speciation in soft-water lakes and soils as determined by EXAFS spectroscopy and geochemical modelling. Geochim. Cosmochim. Acta 2013, 105, 172−186. (48) Harris, W. R. Iron Chemistry. In Molecular and Cellular Iron Transport; Templeton, D. M., Ed.; Marcel Dekker, Inc.: New York, 2005; pp 1−40. (49) Chen, J.; Gu, B.; Royer, R. A.; Burgos, W. D. The roles of natural organic matter in chemical and microbial reduction of ferric iron. Sci. Total Environ. 2003, 307, 167−178. (50) Bauer, I.; Kappler, A. Rates and extent of reduction of Fe(III) compounds and O2 by humic substances. Environ. Sci. Technol. 2009, 43, 4902−4908. (51) Jiang, J.; Bauer, I.; Paul, A.; Kappler, A. Arsenic redox changes by microbially and chemically formed semiquinone radicals and hydroquinones in a humic substance model quinone. Environ. Sci. Technol. 2009, 43, 3639−3645. (52) Chemical Properties of IHSS Samples http://www. humicsubstances.org/ (accessed May 11, 2014). (53) Gustafsson, J. P.; Persson, I.; Kleja, D. B.; Van Schaik, J. W. J. Binding of iron(III) to organic soils: EXAFS spectroscopy and chemical equilibrium modeling. Environ. Sci. Technol. 2007, 41, 1232− 1237. (54) Jones, A. M.; Griffin, P. J.; Waite, T. D. Ferrous iron oxidation by molecular oxygen under acidic conditions: The effect of citrate, EDTA and fulvic acid. Geochim. Cosmochim. Acta 2015, 160, 117−131. (55) Rizvi, M. A.; Syed, R. M.; Khan, B. Complexation effect on redox potential of Iron(III) - Iron(II) couple: A simple potentiometric experiment. J. Chem. Educ. 2011, 88, 220−222. (56) Rizvi, M. A. Complexation modulated redox behavior of transition metal systems (review). Russ. J. Gen. Chem. 2015, 85, 959− 973. (57) Vairavamurthy, A.; Wang, S. Organic nitrogen in geomacromolecules: Insights on speciation and transformation with Kedge XANES spectroscopy. Environ. Sci. Technol. 2002, 36, 3050− 3056. (58) Ritchie, J. D.; Michael Perdue, E. Proton-binding study of standard and reference fulvic acids, humic acids, and natural organic matter. Geochim. Cosmochim. Acta 2003, 67, 85−93. (59) Thorn, K. A.; Folan, D. W.; MacCarthy, P. Characterization of the

International Humic Substances Society Standard and Reference Fulvic and Humic Acids by Solution State Carbon-13 (13C) and Hydrogen-1 (1H) Nuclear Magnetic Resonance Spectrometry; Water Resources Investigations Report 89-4196; Denver, CO, 1989. (60) Hem, J. D.; Cropper, W. H. Survey of Ferrous-Ferric Chemcial Equilibria and Redox Potentials; Water-Supply Paper 1459; Washington, 1962. (61) Roginsky, V.; Barsukova, T. Kinetics of oxidation of hydroquinones by molecular oxygen. Effect of superoxide dismutase. J. Chem. Soc. Perkin Trans. 2 2000, 1575−1582. (62) Rose, A. L.; Waite, T. D. Reduction of organically complexed ferric iron by superoxide in a simulated natural water. Environ. Sci. Technol. 2005, 39, 2645−2650. (63) Yuan, X.; Davis, J. A.; Nico, P. S. Iron-mediated oxidation of methoxyhydroquinone under dark conditions: kinetic and mechanistic insights. Environ. Sci. Technol. 2016, 50, 1731−1740. (64) Lovley, D. R.; Coates, J. D.; Blunt-Harris, E. L.; Phillips, E. J. P.; Woodward, J. C. Humic substances as electron acceptors for microbial respiration. Nature 1996, 382, 445−448. (65) Lovley, D. R.; Fraga, J. L.; Blunt-Harris, E. L.; Hayes, L. A.; Phillips, E. J. P.; Coates, J. D. Humic Substances as a Mediator for Microbially Catalyzed Metal Reduction. Acta Hydrochim. Hydrobiol. 1998, 26, 152−157.